

A scalable and highly immunogenic virus-like particle-based vaccine against SARS-CoV-2

Mona Mohsen¹, Ina Balke², Simon Zinkhan¹, Villija Zeltina², Xuelan Liu¹, Xinyue Chang¹, Pascal S. Krenger¹, Kevin Plattner¹, Zahra Gharailoo¹, Anne-Cathrine S. Vogt¹, Gilles Augusto¹, Marianne Zwicker¹, Salony Roongta¹, Dominik A. Rothen¹, Romano Josi¹, Joana J. da Costa¹, Jan M. Sobczak¹, Aleksandra Nonic¹, Lee-Anne Brand¹, Katja Nuss³, Byron Martina⁴, Daniel E. Speiser¹, Thomas Kündig⁵, Gary T. Jennings⁶, Senta M. Walton⁶, Monique Vogel¹, Andris Zeltins², and Martin Bachmann¹

¹Inselspital Bern Universitätsklinik für Rheumatologie Immunologie und Allergologie

²Latvijas Biomedicīnas pētījumu un studiju centrs

³Vetsuisse-Fakultät an der Universität Zürich

⁴Erasmus Universiteit Rotterdam Departement Econometrie

⁵UniversitätsSpital Zürich Dermatologische Klinik

⁶Citibank Switzerland AG

July 18, 2021

Abstract

SARS-CoV-2 caused one of the most devastating pandemics in the recent history of mankind. Due to various countermeasures, including lock-downs, wearing masks and increased hygiene, the virus has been controlled in some parts of the world. More recently, the availability of vaccines, based on RNA or Adenoviruses, have greatly added to our ability to keep the virus at bay, again in some parts of the world only. While available vaccines are effective, it would be desirable to also have more classical vaccines at hand for the future. Key feature of vaccines for long-term control of SARS-CoV-2 would be inexpensive production at large scale, ability to make multiple booster injections and long-term stability at +4 °C. Here we describe such a vaccine candidate, consisting of the SARS-CoV-2 receptor binding motif grafted genetically onto the surface of the immunologically optimized cucumber mosaic virus, called CuMV_{TT}-RBM. Using bacterial fermenter production and continuous flow centrifugation, the productivity of the production process is estimated to be >2.5 million doses per 1000 liter fermenter run and the vaccine candidate is stable for at least 14 months at 4°C. We further demonstrate that the candidate vaccine is highly immunogenic in mice and rabbits and induces more high avidity antibodies compared to convalescent human sera and antibodies induced are more cross-reactive to mutant RBDs for variants of concern (VoC). Furthermore, antibody responses are neutralizing and long-lived. This, the here presented VLP-based vaccine may be a good candidate for use as conventional vaccine in the long-term.

Introduction

Since the outbreak of the global pandemic caused by SARS-CoV-2, WHO has reported ~170 million confirmed cases on June third 2021 including 3.5 million deaths (WHO, June 3rd 2021). The pandemic has put a heavy toll on public health systems and world's economy. To limit the damage, efforts have been directed towards vaccine development. On 12th May 2021 around one billion doses of different vaccines have been administered worldwide (WHO, 12th May 2021). Although SARS-CoV-2 causes mostly mild symptoms such as coughing, fever and breathlessness, symptoms may become much more severe, in particular in elderly people and people with chronic diseases which may develop severe pneumonia and other symptoms including organ failure and

death (1, 2). In comparison to SARS-CoV-1 and MERS-CoV, SARS-CoV-2 causes less morbidity; however, it transmits much more readily, mostly because non-symptomatic and pre-symptomatic individuals can spread the virus. Thus, while MERS-CoV and SARS-CoV outbreaks have been sporadic and geographically restricted, SARS-CoV-2 has rapidly spread around the world (3, 4).

The positive sense ssRNA SARS-CoV-2 virus has a genome of about 29,700 nucleotides with 79.5% identity to SARS-CoV-1. Its genome encodes four main structural proteins; spike (S) protein, membrane (M) protein, nucleocapsid (N) protein as well as the envelope (E) protein (5, 6). SARS-CoV-2 binds to angiotensin converting enzyme 2 (ACE2) via the RBD domain of its S protein that protrudes from the viral envelope. Interaction of RBD with ACE2 is the first step in a cascade of event leading to viral entry and ultimately replication (7). Neutralizing antibodies against SARS-CoV-2 are mostly targeting the receptor binding domain (RBD) of the S protein. Within RBD, the receptor binding motif (RBM) is of particular importance as it directly interacts with ACE2 (8). Compared to SARS-CoV-1, the affinity to ACE2 of the S protein expressed by the original variant of SARS-CoV-2 is about 4-fold higher, offering an explanation for the increased infectivity of the latter (9). Interestingly, RBM shows no glycosylation or other post-translational modifications and therefore is well suited for production in bacterial expression systems (10).

Vaccines are the most reliable, cost-effective and efficient strategy to prevent infectious diseases. Vaccine candidates must induce sufficient quantities of high affinity antibodies to neutralize the invading virus. Since the initiation of the pandemic, a full spectrum of vaccine types has been tested in preclinical and clinical trials. Vaccine platforms employed mRNA, DNA, viral vectors, inactivated or live-attenuated virus (9, 11) and recombinant proteins. The full-length of S protein, the RBD domain, S1 subunit, fusion protein (FP) as well as the N-terminal domain (NTD) of the S protein have been targeted by vaccines that are licensed or undergoing development (3, 12).

Virus-like particles (VLPs) represent one of the conventional vaccine platforms in the sense that there are globally marketed products (e.g., HBV and HPV vaccines) that have demonstrated the clinical usefulness of this modality. VLPs consist of viral structural proteins that upon recombinant expression, self-assemble into particles with a mostly icosahedrons and rarely helical symmetry (13). Recently, we have developed an immunologically optimized VLP platform based on the cucumber mosaic virus (CuMV_{TT}-VLPs) (14). CuMV_{TT} VLPs incorporate a universal T cell epitope derived from tetanus toxin (TT) utilizing the pre-existing T cell memory response induced by vaccination against tetanus toxin (15). The newly developed platform enhances the interaction between T helper cells and B cells, and is expected to improve responses in elderly individuals who are often less reactive to vaccines. This is supported by the fact that pre-existing immunity to the chosen TT epitope is very broad in humans (and animals) as the peptide binds to essentially all HLA-DR molecules and most people have been immunized many times against TT. In addition, the CuMV_{TT}-VLPs are packaged with bacterial RNA which is a ligand for toll like receptor (TLR) 7 and 8 and serves as a potent adjuvant (15, 16). By displaying antigens on CuMV_{TT}-VLPs, it was possible to induce high levels of antigen-specific antibodies in mice, rats, cats, dogs and horses and treat diseases such as atopic dermatitis in dogs or insect bite hypersensitivity in horses (17, 18).

In the current study, we have designed and developed a scalable and immunogenic VLP-based COVID-19 vaccine by genetically fusing the RBM domain of the S protein from SARS-CoV-2 into CuMV_{TT}-VLPs. The data shows that this vaccine is highly immunogenic inducing both RBD-specific IgG and IgA antibodies as well as a strong viral neutralizing antibody response. Furthermore, the vaccine production process is highly scalable, potentially allowing the production of millions of doses in a single 1000L fermenter run.

Results:

CuMV_{TT}-VLPs constitute an efficient platform for genetically fusing the receptor-binding domain (RBM)

Our first attempt to generate a COVID-19 vaccine using CuMV_{TT} VLPs platform, utilized recombinant RBD which was chemically coupled to the VLPs using SMPH cross-linker (19). This method resulted in a vaccine candidate that binds ACE2 and induces high levels of RBD-specific antibodies which were able to

strongly inhibit RBD binding to ACE2 and neutralize SARS-CoV-2/ABS/NL20 virus (20).

In an attempt to produce a more readily scalable vaccine-candidate with better yield, we genetically fused RBM domain into CuMV_{TT} to produce a mosaic vaccine as illustrated in Figure 1A. The mosaic vaccine (mCuMV_{TT}-RBM) consists of both unmodified and a genetically modified monomer spontaneously assembling in *E. coli* to form VLPs. The genetically modified monomer displays RBM domain on the exterior surface. mCuMV_{TT}-RBM was expressed and produced in *E. coli*. In contrast, incorporating either the RBD or RBM into all VLP coat protein subunits was not successful and resulted in formation of coat protein aggregates and insoluble VLPs (data not shown). Purification of mCuMV_{TT}-RBM was carried out by ultracentrifugation using a 20-60% sucrose gradient (Fig. 1B). We have shown previously that using *E. coli* as an expression system facilitates packaging of prokaryotic ssRNA which serves as a TLR7/9 ligand and results in an enhanced immune response (16, 21) (Fig. 1C). The final product mCuMV_{TT}-RBM consists of an unmodified VLP coat protein monomer of ~28 kDa in size while the genetically modified one is ~42 kDa as shown in the SDS-PAGE (Fig. 1D). Densitometric analysis suggested 40-50% incorporation of coat protein-RBM fusion molecules into the VLPs. As each VLP contains 180 capsid proteins, 40-50% RBM means that each VLP has about 70-90 RBM antigens. Electron microscopy confirmed the successful assembly of icosahedral mCuMV_{TT}-RBM into $T=3$ particles with no sign of aggregation or malformation of the particles (Fig. 1E). Dynamic light scattering revealed a uniform and homogenous peak of hydrodynamic diameter (DH) of ~94nm (Fig. 1F).

An ideal vaccine would have a long shelf life at ambient temperatures, nevertheless many commercial vaccines require storage temperatures between 2-4°C (22). Whilst maintaining a vaccine in a cold chain below freezing temperature can be difficult in developed countries, it is particularly challenging and sometime prohibitive for developing countries (23). Accordingly, we tested the stability of our vaccine candidate. The results indicated that the vaccine is stable for 14 months at 4°C and for approximately 1 month at RT (Supplementary Fig.1).

As mentioned above, RBM is the part of the RBD, which is responsible for the binding of the virus to the receptor ACE2. It is also the major site of neutralizing antibody epitopes. To confirm the native conformation of RBM in the context of the mosaic fusion VLP, we tested whether the vaccine was able to bind to ACE2. To this end, the human receptor ACE2 was coated onto an ELISA plate. The candidate vaccine or a control CuMV_{TT} VLP without an RBM insertion were then added and anti-CuMV_{TT} secondary antibodies used to detect receptor bound VLPs. The results confirmed that mCuMV_{TT}-RBM vaccine can bind to ACE2 receptor indicating that RBM exhibits the right native conformation(s) on the surface of the VLPs. The control did not show any binding (Fig. 1G).

mCuMV_{TT}-RBM induces high levels of specific antibodies with high avidity against RBD and Spike proteins of SARS-CoV-2

Next, we investigated the immunogenicity of mCuMV_{TT}-RBM *in vivo*. We have tested different doses and vaccination regimens (Fig. 2A). We concluded that priming with 100 µg on day 0 followed by a booster dose of 100 µg on day 28 induces the best antibody titers. Accordingly, BALB/cOlaHsd mice were s.c. immunized using this dose and regimen. No adjuvants have been added as the vaccine is self-adjuvanted with the prokaryotic ssRNA packaged during the expression process (14). The collected sera were tested for the induction of antibodies against RBD and spike protein of SARS-CoV-2. The results revealed a successful induction of anti-RBD IgGs; seven days following the priming dose which continued to increase steadily. The booster dose has significantly augmented the response by approximately ten-fold (Fig. 2B and C). Antibody response against the spike protein has also been detected following the priming dose albeit to a lower extent, compared to RBD. However, the response increased dramatically following the booster dose (Fig. 2D and E). The avidity of an antibody is defined as the binding strength through points of interaction with the cognate antigen. It can be quantified as the ratio of the dissociation constant K_d for the intrinsic affinity over the one for the functional affinity of an antibody (24). Avidity and functional affinity terms can be exchanged in a looser sense (25). We have performed a modified immunoassay using 7M urea to detach low avidity antibodies. More specifically, we have compared the avidity of the antibodies in sera collected on day 42, after immunization with 100 µg on day 0 and boosting with 100 µg on either day 14 (D0/14

regimen) or 28 (D0/28 regimen). The results revealed that ~50% of the induced RBD-specific antibodies are of high avidity when using D0/28 vaccination regimen versus ~20% only for D0/14 regimen ($p = 0.0008$) (Fig. 2F-H). Similar findings have been seen for spike-specific antibodies ($p = 0.0144$) (Supplementary Fig. 2 A-C). Some studies showed that neutralizing antibodies against SARS-CoV-2 wane relatively rapidly (26) and some patients may even completely lack long-lasting SARS-CoV-2 antibodies (27). It was therefore of interest to assess the longevity of antibodies induced after vaccination with mCuMV_{TT}-RBM. Accordingly, we have tested RBD- and spike-specific IgG antibodies 134 days following priming. The results revealed that the antibody titers remained stable and comparable to the titer achieved on day 42 after boost (Fig. 2I and J).

mCuMV_{TT}-RBM was tested in rabbits (males and females) to evaluate the immunogenicity and toxicity (tolerability) of the vaccine candidate. Rabbits were vaccinated intramuscularly (i.m.) on day 0 and received booster doses on days 14 and 28. Sera collected on day 42 have shown a strong increase in RBD-specific antibodies (around OD₅₀ of 1:10000) (Supplementary Fig. 3). Toxicology studies demonstrated no evidence of clinical signs or systemic toxicity resulting from multiple administrations of mCuMV_{TT}-RBM vaccine candidate. A mild influx of inflammatory cells at the injection site was observed.

mCuMV_{TT}-RBM promotes IgA production and IgG responses are dominated with IgG2a subclass

Previous studies have shown that the different IgG subclasses play an essential role against viruses by complement fixation, enhancing opsonization and immune effector function (28). Accordingly, it is of interest to assess the IgG subclasses induced by the developed vaccine candidate. We have tested the vaccine for its ability to induce IgG1, IgG2a, IgG2b and IgG3. The results indicated that mCuMV_{TT}-RBM induces the production of all four subclasses when binding is assessed on RBD protein as shown in Figure 3A and B. Analysis of OD₅₀ showed a predominance of IgG2a and IgG1. These results were confirmed when assessing the binding to the spike protein (Fig 3C and D).

Next, we tested the ability of mCuMV_{TT}-RBM to induce immunoglobulin class-switching to IgA using the two regimens D0/14 and D0/28. Following, D0/28 regimen induced higher RBD-specific IgA titers in comparison to D0/14 regimen (Fig. 3E). Measuring the OD₅₀ of IgA titers in both regimens confirmed the difference in antibody titers (Fig. 3F).

Recognition of SARS-CoV-2 variants of concern

We have previously produced a number of RBD's variants, including the UK, Brazilian and Indian VOC (29, 30) and shown, as others, that mutations at position E484K strongly reduce recognition by convalescent sera (30, 31). It is therefore of significant interest that our vaccine induced immune sera recognized all variant RBDs equally well as the wild type RBD (Fig 4A and B). Hence, this vaccine candidate may have the potential to protect against all VoC that occurred up to now equally well.

mCuMV_{TT}-RBM induces higher antibody titers in comparison to SARS-CoV-2 convalescent sera

In comparison to infections with other viruses, patients infected with COVID-19 produce neutralizing antibodies at relatively low levels (27, 32). Hence, we compared the total RBD-specific IgG titer induced in mouse sera after vaccination with mCuMV_{TT}-RBM to SARS-CoV-2 convalescent sera (total of 5 different sera). The results showed that the vaccine induces higher RBD-specific antibody titers even after a single priming dose compared to natural infection with SARS-CoV-2 and the booster injection further increased the RBD-specific antibody responses (Fig. 5A and B). Analysis of Area Under Curve (AUC) indicated a high difference ($p < 0.0001$) between mouse sera collected on day 14 (after priming) or day 42 (after boost) to convalescent sera (Fig. 5C and D).

Administration of a second booster dose further enhances antibody response and neutralization capacity of mCuMV_{TT}-RBM

In a next step, we compared the efficacy of vaccinating mice with a total of 2 doses of mCuMV_{TT}-RBM (Prime/Boost) versus 3 doses (Prime/Boost/Boost) as illustrated in Figure 6A.

The results showed no significant difference in the induced RBD-specific antibody titers following the 2nd dose in comparison to sera following the 3rd dose (Fig. 6B and C). Furthermore, the avidity of the induced antibodies induced after the 3rd dose did not show a higher value when compared to the ones induced following the 2nd dose (Fig. 6D and E).

To test the capacity of the induced antibodies to neutralize the real virus, we have performed cytopathic effect (CPE) using 100 TCID₅₀ of SARS-CoV-2/ABS/NL20. Titers are expressed as the highest dilution that inhibits formation of CPE 100%. In contrast to ELISA titers, a significant difference in neutralization capacity was seen when comparing day 42 sera of vaccinated mice vs the control group ($p = 0.0014$). However, sera from mice after the 3rd dose of the vaccine (day 63) showed further enhanced neutralization titer when compared to the control group ($p < 0.00001$) or the group received only the 2nd dose ($p = 0.0021$) (Fig. 6F). The obtained results show the capacity of the vaccine candidate to completely block the cytopathic effect of the virus.

Efficient upscaling of mCuMV_{TT}-VLPs vaccine candidate

Manufacturability, in particular scalability and production yield, is a critical attribute in selecting vaccine candidates to address a global pandemic. For this reason, we focused from the beginning on a VLP-based vaccine that can be efficiently produced in bacteria. Indeed, as the RBM of SARS-CoV-2 is not glycosylated and has no other posttranslational modifications, it may be an optimal candidate for a VLP-based vaccine candidate produced in *E. coli*.

Continuous flow ultracentrifugation is a method used to produce >80% of the annual global influenza vaccine inventory which is approximately 1.5 billion doses (33). Continuous flow ultracentrifugation is thus an ideal and an established method for purification at large scale. To assess the potential yields of our production process, we produced a batch of mCuMV_{TT}-RBM in a 2litre fermenter and purified the resultant VLPs by continuous flow ultracentrifugation (Fig 7A). SDS PAGE analysis showed good incorporation of RBM and EM-analysis showed well-formed particles (Fig. 7B-D). The process yield from 2L of fermentation volume was approximately 0.5 g. This would correspond to 2.5 mio doses produced in a single 1000-liter fermentation run. As this process is not optimized, there is the potential to significantly improve the already impressive yield.

Discussion:

In the current study, we investigated a novel VLP-based vaccine for COVID-19. Specifically, we have generated a mosaic VLP-vaccine using the plant-derived cucumber-mosaic VLPs (CuMV_{TT}). Mosaic VLPs are well known in the field with GSKs RTS, S malaria vaccines as the most prominent member of the field (34). The mosaic vaccine candidate consists of an unmodified monomer and a genetically modified monomer that incorporates the RBM domain of SARS-CoV-2. The RBM domain was chosen as the target epitope due to the fact that RBD/RBM are considered the immunological Achilles' heel of SARS-CoV-2 and unlike RBD, RBM domain does not show any glycosylation, likely facilitating protein-protein interaction with ACE2 (10, 35, 36). Furthermore, incorporating the whole RBD domain into CuMV_{TT} did not allow the formation of VLPs most likely due to steric constraints. The used genetic fusion technique in this study facilitated the assembly of $T=3$ icosahedral VLPs which is essential for effective induction of a humoral immune response (13). Using this technique, we have recently developed a vaccine against MERS-CoV by incorporating the RBM domain into CuMV_{TT}. The developed vaccine induced antibodies that completely neutralized MERS-CoV/EMC/2012 isolate (manuscript in press). Furthermore, we have shown that fusing RBM domain into AP205-VLPs results in an effective vaccine which induced RBD and spike-antibodies and was capable of neutralizing the wild type virus SARS-CoV-2/ABS/NL20 (37). Development of AP205-RBM vaccine required a refolding process which typically results in lower amounts of correctly folded target protein, and may be distinguished from re-assembly processes used for HPV and HEV vaccines (38). The simplicity of the downstream processing at industrial scale is therefore a major advantage of the current

vaccine candidate.

Using CuMV_{TT}-VLPs as a vaccine platform resulted in a soluble VLP. The SDS-PAGE analysis indicated 40-50% incorporation of RBM domain. Using Sandwich ELISAs, we have shown that the mCuMV_{TT}-RBM vaccine is able to detect and bind to the viral receptor ACE2. This confirms that the RBM domain displayed and fused to the VLP, has the correct conformation which is essential for the induction of the appropriate neutralizing antibody response. Expression in *E. coli* facilitates the packaging of bacterial RNA which serves as TLR7/8 ligand. We have shown previously that VLP-based vaccines are capable of inducing IL-21 independent secondary plasma cells only in the presence of TLR7/8 agonist such as bacterial ssRNA (16, 21). Additionally, TLR7/8 agonist polarizes the immune response towards T_H1 and cytotoxic T cells which is essential to avoid enhanced disease as shown in preclinical challenge models (9). A recent study has shown that IgA antibodies in serum, saliva as well as bronchoalveolar lavage dominated the early response against SARS-CoV-2 infection in comparison to IgG and IgM. Sterlin *et al* , have also shown that IgA serum are more potent in neutralizing wild type SARS-CoV-2 than IgG (39). RNA loaded VLPs may also induce IgA responses, again in a TLR7/8 dependent manner (16, 40). This appears particularly important for SARS-CoV-2 and other respiratory diseases-causing viruses, such as SARS-CoV-1 and MERS-CoV-2, as IgA may be able to neutralize the virus locally in the lung without causing inflammation, a feature that may be particularly critical in patients with high viral load (41). Thus, it is therefore of key importance that our newly developed vaccine is able to induce a significant increase in serum IgA levels. Whether the increased serum IgA levels in mice can translate to correspondingly high IgA levels in humans and in particular at mucosa sites needs to be confirmed.

We have also shown that mCuMV_{TT}-RBM vaccine candidate is strongly immunogenic in mice and rabbits. The response was further augmented following the booster dose. Using a D0/28 vaccination regimen induced a better quality of RBD and spike-protein antibodies in comparison to D0/14 regimen. This may indicate that it takes longer to induce such high-affinity/avidity antibodies as demonstrated here by mCuMV_{TT}-RBM.

It has been shown that the induced neutralizing antibody response in SARS-CoV-2 patients are of low and short duration (27, 32). This may be explained by coronaviruses morphological structure which are large particles with long spike proteins exhibiting RBD trimers spaced by 25 nm. Other viruses as well as virus-like particles (VLPs) are capable of inducing optimal and long-lived neutralizing antibodies thanks to the 180 monomers forming a repetitive surface structure with epitopes spaced by 5-10 nm (27). The induced antibodies using mCuMV_{TT}-RBM vaccine candidate could be detected in a similar level 4 months following the priming boost in the immunized mice sera. Furthermore, the main goal of any-viral vaccine is the induction of neutralizing antibodies that can inhibit SARS-CoV-2 infection. Our test sera were probed for their ability to inhibit a cytopathic effect (CPE) of wild-type SARS-CoV-2 isolate on Vero cells. The neutralizing capability of the virus was further enhanced following a 3rd dose.

We have shown recently that N501Y mutation enhanced the binding affinity to ACE2 but did not significantly affect the recognition of RBD by convalescent sera, which was not the case for E484K mutation that resulted in abolished the recognition (42). mCuMV_{TT}-RBM is shown here to induce antibodies of much higher affinity/avidity than SARS-CoV-2 typically does in humans. This increased affinity/avidity translates to increased cross-reactivity with SARS-CoV-2 VoC. Indeed, antibodies induced by the here presented vaccine candidate recognizes variant strains of concern from Brazil, UK and India with equal efficiency suggesting that our vaccine can protect against the new variants. In addition, the vaccine candidate may be stored at 4°C for at least a year, representing in addition to the very high production yields and immunogenicity, two additional key assets of mCuMV_{TT}-RBM.

Collectively, we have shown in this study that this novel mosaic VLP-based vaccine can efficiently induce high specific anti-RBD and spike antibodies that effectively neutralize SARS-CoV-2 and highly cross-reacts with all emerging viral VoC tested. As COVID-19 continues to represents a global threat to human health, it seems rational to further develop this vaccine candidate.

Methods:

Mosaic CuMV_{TT}-RBM vaccine production, purification and analysis

For expression and purification of mosaic CuMV_{TT}-RBM, *E. coli* C2566 (New England Biolabs, USA) competent cells were transformed with the plasmid pETDu-CMVB3d-nCoV-M-CMVtt.

After selection of clones with the highest expression level of target proteins, *E. coli* culture was grown in 100 ml of 2TY medium (1.6% trypton, 1% yeast extract, 0.5% NaCl, 0.1% glucose) containing ampicillin (100 mg/l) on an orbital shaker at 30°C to the OD(600) value of 0.8–1.0. Then, the cells were induced with 0.2mM IPTG, and the medium was supplemented with 5mM MgCl₂. Incubation was continued on the rotary shaker (200 rpm, 20°C, 18h). The resulting biomass was collected by low-speed centrifugation and was frozen at -20°C. To disrupt the cells, the biomass was resuspended 10 ml of buffer (20mM Tris, 5mM EDTA, 5mM Et-SH, 5% glycerol, 10% sucrose, pH 8.0) and further treated with ultrasound (Hielscher 200, power 70%, pulse 50%, 16min) on ice. Then, 0.5% TX-100 was added and the solution was rotated at 10 rpm ON at 4°C without centrifugation. The solution was then clarified for 10min at 10000 rpm (Eppendorf 5804) and the pellet was discarded. The soluble fraction was loaded on the top of the sucrose gradient (20-60%; in buffer containing 20mM Tris, 2mM EDTA, 5% glycerol, 0.5% TX-100, pH 8.0) and centrifugated in Beckman SW32 rotor for 6h at 25500 rpm at 18°C. The gradient fractions (6 ml) were then removed from the bottom of the 38 ml tube. The CuMV VLP containing fraction (40 and 50% sucrose, pooled) was diluted 1:1 with buffer (20mM Tris, 2mM EDTA, 5% glycerol, pH 8.0). The VLPs were sedimented using Type 70 rotor (Beckman, 50000 rpm, 4h, 4°C). Then the pellet was dissolved ON in 4 ml of 20mM Tris, 2mM EDTA at 4°C. The solution was clarified by centrifugation (5min, 14000 rpm), the clarified solution overlaid on top of the 30% sucrose „cushion“ solution in 20mM Tris, 2mM EDTA, 0.5% TX-100, pH 8.0. The VLPs were sedimented using Beckman TLA100.3 rotor (72000 rpm, 60min, 4degC). The pellet was solubilized in 2 ml of 20mM Tris, 2mM EDTA and clarified again by centrifugation (5min, 14000 rpm). Obtained VLPs were characterized using SDS-PAGE, agarose gel, electron microscopy and dynamic light scattering. Protein concentration was determined using BCA test.

Dynamic light scattering

Sample VLP solution (1 mg/ml) was analyzed on a Zetasizer Nano ZS instrument (Malvern Instruments Ltd, UK). The results of three measurements were analyzed by DTS software (Malvern, version 6.32) (15).

Electron microscopy

Physical stability and integrity of the mosaic CuMV_{TT}-RBM were visualized by transmission electron microscopy (Philips CM12 EM). For imaging, sample-grids were glow discharged and 2µl of purified CuMV_{TT}-RBM (3mg/ml) was added for 30s. Grids were washed 3x with ddH₂O and negatively stained with 5 µl of 5% uranyl acetate for 30s. Excess uranyl acetate was removed by pipetting and the grids were air dried for 10min. Images were taken with 84,000x and 110,000x magnification.

Binding ELISA assay

To test if the vaccine can bind the relevant human receptor ACE2, the plates were coated with 1µg/ml of ACE2 in PBS at a volume of 50µl/well. The plate was incubated at 4°C overnight. The plate was washed with PBS, Tween 0.01%. Added 50µl/well of Superblock solution (Thermo Fisher, 37518) and incubated for 1h at RT on a shaker. The blocking solution was flicked off and 50µl of the CuMV_{TT}-RBM or CuMV_{TT}-VLPs at 1µg/ml were added to the first row of the plate followed by 1:3 dilution. The plate was incubated for 1h at RT, washed with PBS+Tween 0.01%. 50µl of mouse anti-CuMV_{TT} monoclonal antibody (clone 1-1A8/ batch 2) at a concentration of 1µg/ml was added to each well as a secondary antibody and incubated for 1h at RT on a shaker. The plate was washed and 50µl of the detection antibody; HRP labelled goat anti-mouse IgG Fc gamma at a dilution of 1:1000 in PBS-Casein 0.15% was added to each well. The plate was incubated for 1h at RT. The plate was developed and OD₄₅₀ reading was performed (BioTek, USA).

Mice

In vivo experiments were performed using 8-12 weeks-old female, BALB/cOlaHsd wild-type (wt) mice pur-

chased from Harlan (Netherlands). All animal procedures were conducted in accordance with the Swiss Animal Act (455.109.1 – September 2008, 5th) of University of Bern. All animals were treated for experimentation according to protocols approved by the Swiss Federal Veterinary Office.

Rabbits

A toxicology study was performed in rabbits according to ICH guidelines for the preclinical safety evaluation of vaccines and the preclinical pharmacological and toxicological testing of vaccines. Studies were performed according to the principles of good laboratory practice at the Musculoskeletal Research Unit (MSRU) of the Vetsuisse Faculty of the University of Zürich.

Human sera

Human sera were obtained from 5 COVID-19 convalescent patients which were recruited at the University Hospital of Bern, Bern, Switzerland as described (43). Participants were recruited via three different routes: (a) inpatients with a SARS-CoV-2 test result (real-time PCR; RT-PCR), (b) medical personnel of the Inselspital, and (c) residual material from patients stored at the Liquid Biobank Bern (www.biobankbern.ch). Inclusion criteria of inpatients are (a) hospitalization in Inselspital, (b) tested positive for SARS-CoV-2 using RT-PCR (nasopharyngeal swab), (c) aged 18 or older, and (d) signed general consent.

Vaccination regimen/dose/sera collection

Wild type BALB/cOlaHsd mice were vaccinated subcutaneously (s.c.) using different regimens and doses. After comparing the efficacy of the different regimens and doses, 100 μ g of the vaccine or a control (CuMV_{TT}-VLPs, do not display an epitope) was used in the experiments showed in this study. 100 μ g (Prime on day 0) and 100 μ g for a booster dose on day 14 or 28 were used. CuMV_{TT}-RBM candidate vaccine was diluted in 20 mM Tris, 2 mM EDTA in a final volume of 100 μ l for final injection. Serum was collected on a weekly basis. Three doses regimen of each 100 μ g were given at days 0, 28 and 42.

RBD mutations protein expression and purification

SARS-CoV-2 RBD_{wildtype}, RBD_{K417N}, RBD_{E484K}, RBD_{N501Y}, RBD_{K417N/E484K/N501Y}, RBD_{L452R/E484Q} were cloned as a synthetic gene into pTWIST-CMV-BetaGlobin-WPRE-Neo vector (Twist Biosciences, CA, USA) and expressed in HEK293F cells through the Expi293 system (ThermoFisher Scientific, MA, USA). Purification was performed by IMAC using a HiTrap TALON crude column (Cytiva, Uppsala, Sweden).

Enzyme-linked immunosorbant assay (ELISA)

To determine the total IgG antibodies against the candidate vaccine mCuMV_{TT}-RBM in sera of vaccinated mice, ELISA plates were coated with SARS-CoV-2 RBD wildtype or with SARS-CoV-2 Spike (Sinobiological, Beijing, China) at concentrations of either 1 μ g/ml or 0.1 μ g/ml overnight. ELISA plates were washed with PBS-0.01% Tween and blocked using 100 μ l PBS-Casein 0.15% for 2h in RT. Sera from vaccinated mice serially diluted 1:3 starting with a dilution of 1:20 and incubated for 1h at RT. After washing with PBS-0.01%Tween, goat anti-mouse IgG conjugated to Horseradish Peroxidase (HRP) (Jackson ImmunoResearch, West Grove, Pennsylvania) was added at 1/2000 and incubated for 1h at RT ELISA was developed with tetramethylbenzidine (TMB), stopped by adding equal 1 M H₂SO₄ solution, and read at OD₄₅₀ nm or expressed as Log OD₅₀. Detecting RBD-specific IgGs against mutated RBDs was carried out in a similar way.

IgG subclasses were measured from sera collected on day 42 following the same described ELISA protocol. The following secondary antibodies were used: goat anti-mouse IgG1-HRP and goat anti-mouse IgG2a-HRP (1:1000) (Thermo Fischer Scientific, Waltham, Massachusetts), goat anti-mouse IgG2b-HRP (SouthernBiotech, Birmingham, Alabama) 1:4000, rat anti-mouse IgG3-HRP (Becton, Dickinson, Franklin Lakes, New Jersey) 1:2000.

To detect IgA antibodies the plates were coated with 1 μ g/ml SARS-CoV-2 RBD wildtype protein and goat

anti-mouse IgA POX (ICN 55549, ID 91, 1:1000 dilution) as the secondary antibody was used. An additional step prior to serum incubation was added in order to deplete IgG. 10 μ l of Protein G beads (Invitrogen, USA) were transferred into a tube and placed into a magnet. The liquid was removed and the 75.6 μ l diluted sera in PBS-Casein 0.15% was added to the beads and mixed. The tube was incubated on a rotator at RT for 10 minutes. The tubes were placed back into the magnet and ELISA was carried out as described above. Analysis and graphs were created using GraphPad PRISM 9, Version 9.1.0 (216), March 15, 2021.

To determine RBD-specific IgG antibodies against the candidate vaccine mCuMV_{TT}-RBM in sera of vaccinated rabbits, ELISA plates were coated with 2 μ g/ml SARS-CoV-2 RBD_{wildtype} in PBS overnight at +4°C. ELISA plates were washed 4 times with PBST (1x PBS / 0.05 % (v/v) Tween 20) and plates were blocked with 200 μ L/well Blocking buffer (ThermoFisher, Life Technologies Europe BV, Zug Switzerland). Plates were incubated at +22°C between 2-4 h. After removal of the blocking buffer and a washing step, diluted internal standard (1 μ g/mL) and the pre-diluted immune sera (1:50) were added to the wells of the first column on the ELISA plate (150 μ L/well). The internal standard and the immune sera were then serially 3-fold diluted in dilution buffer (2% BSA/ PBST). Plates were incubated for 2 h at +22°C and washed. 100 μ L/well of detection antibody (1:10'000 diluted in dilution buffer, Peroxidase-conjugated polyclonal goat anti- rabbit IgG (H+L) (Jackson Immuno Research, cat no 111-035-144) was added and incubated for 2h at +22°C. After rigorous washing, 100 μ l /well of the OPD detection solution (POD tablets (Sigma cat. no. P6912), phosphate citrate tablets (Sigma cat. no. P4809), 30% H₂O₂ (Sigma cat. No. 1009)) was added and reaction was stopped by addition of 50 μ L/well 2 M H₂SO₄. Absorption at 490 nm was quantified in each well using the plate reader Spark 10M (Tecan).

Avidity (ELISA)

To test IgG antibody avidity against SARS-CoV-2 full spike protein and RBD protein, threefold serial dilutions of 1/20 diluted mice sera, were added to ELISA plates coated over night with 1.0 μ g/ml RBD and spike proteins, respectively. After incubation at RT for 1h, the plates were washed once in PBS-0.01% Tween, and then washed 3x with 7M urea in PBS-0.05%Tween or with PBS-0.05% Tween for 5min every time. After washing with PBS-0.05%Tween, goat anti-mouse IgG conjugated to Horseradish Peroxidase (HRP) (Jackson ImmunoResearch, West Grove, Pennsylvania) was added 1/2000 and incubated for 1h at RT. Plates were developed and read at OD₄₅₀ nm.

Neutralization assay cytopathic effect-based assay (CPE)

To determine the neutralizing ability and capacity of vaccine induced antibodies a CPE assay was performed using wild-type SARS-CoV-2 (SARS-CoV-2/ABS/NL20). Serum samples were heat-inactivated for 30min at 56°C. Two-fold serial dilutions were prepared starting at 1:20 up to 1:160. 100 TCID₅₀ of the virus was added to each well and incubated for 37°C for 1h. The mixture has been added on a monolayer of Vero cells and incubated again for 37°C for 4 days. Four days later the cells were inspected for cytopathic effect. The titer was expressed as the highest dilution that fully inhibits formation of CPE.

Statistical analysis

Data were analyzed and presented as (mean \pm SEM) using *Student's t-test* , One-way ANOVA or Area Under Curve (AUC) as mentioned in the figure legends, with GraphPad PRISM 9. The value of $p < 0.05$ was considered statistically significant (* $p < 0.01$, ** $p < 0.001$, *** $p < 0.0001$).

Continuous flow centrifugation

Bacterial lysates were generated as described in 2.1 and applied to a sucrose gradient in a continuous flow centrifugation (AW Promatix 1000). The fractions obtained were analyzed by SDS PAGE, native agarose gel electrophoresis and electron microscopy.

Acknowledgment

This work was supported by Saiba AG and Inselspital Bern.

Declaration of interests: M. F. Bachmann is a board member of Saiba AG and holds the patent of CuMV_{TT}-VLPs. G. T. Jennings works for Saiba AG.

Data availability statement:

The datasets generated during and/or analyzed during the current study are available from the corresponding author on reasonable request.

Authors Contributions:

Design of experiments, acquisition of data, interpretation and analysis of data: MOM, MFB, AZ, IB, SZ, VZ, XL, XCPSK, KP, ZG, ASV, GA, MZ, SR, DAR, RJ, KN and BM. Writing, revision and editing of manuscript: MOM, AZ, SMW, GTJ, MV, DES and MFB. Technical, material and tool support: LAB, JMS, AN, JJC, DES, MV, MV, MOM, SMW, GTJ, AZ and MFB.

Study supervision: MOM, MV, SMW, GTJ, TK, AZ and MFB. All authors read and approved the final manuscript.

References:

1. Guan WJ, Ni ZY, Hu Y, Liang WH, Ou CQ, He JX, et al. Clinical Characteristics of Coronavirus Disease 2019 in China. *N Engl J Med.* 2020.
2. Amirfakhryan H, Safari F. Outbreak of SARS-CoV2: Pathogenesis of infection and cardiovascular involvement. *Hellenic J Cardiol.* 2021;62(1):13-23.
3. Awadasseid A, Wu Y, Tanaka Y, Zhang W. Current advances in the development of SARS-CoV-2 vaccines. *Int J Biol Sci.* 2021;17(1):8-19.
4. Cevik M, Kuppalli K, Kindrachuk J, Peiris M. Virology, transmission, and pathogenesis of SARS-CoV-2. *BMJ.* 2020;371:m3862.
5. Phan T. Novel coronavirus: From discovery to clinical diagnostics. *Infect Genet Evol.* 2020;79:104211.
6. Bhat EA, Khan J, Sajjad N, Ali A, Aldakeel FM, Mateen A, et al. SARS-CoV-2: Insight in genome structure, pathogenesis and viral receptor binding analysis - An updated review. *Int Immunopharmacol.* 2021;95:107493.
7. Hoffmann M, Kleine-Weber H, Schroeder S, Kruger N, Herrler T, Erichsen S, et al. SARS-CoV-2 Cell Entry Depends on ACE2 and TMPRSS2 and Is Blocked by a Clinically Proven Protease Inhibitor. *Cell.* 2020;181(2):271-80 e8.
8. Lan J, Ge J, Yu J, Shan S, Zhou H, Fan S, et al. Structure of the SARS-CoV-2 spike receptor-binding domain bound to the ACE2 receptor. *Nature.* 2020;581(7807):215-20.
9. Speiser DE, Bachmann MF. COVID-19: Mechanisms of Vaccination and Immunity. *Vaccines (Basel).* 2020;8(3).
10. Casalino L, Gaieb Z, Goldsmith JA, Hjorth CK, Dommer AC, Harbison AM, et al. Beyond Shielding: The Roles of Glycans in the SARS-CoV-2 Spike Protein. *ACS Cent Sci.* 2020;6(10):1722-34.
11. Lane TF, Eber RM, Gansky S, Reddy MS. Vaccines for COVID-19: An Overview. *Compend Contin Educ Dent.* 2021;42(6):298-304; quiz 5.
12. Malik JA, Mulla AH, Farooqi T, Pottoo FH, Anwar S, Rengasamy KRR. Targets and strategies for vaccine development against SARS-CoV-2. *Biomed Pharmacother.* 2021;137:111254.
13. Zinkhan S, Ogrina A, Balke I, Resevica G, Zeltins A, de Brot S, et al. The impact of size on particle drainage dynamics and antibody response. *J Control Release.* 2021;331:296-308.

14. Mohsen MO, Augusto G, Bachmann MF. The 3Ds in virus-like particle based-vaccines: "Design, Delivery and Dynamics". *Immunol Rev.* 2020.
15. Zeltins A, West J, Zabel F, El Turabi A, Balke I, Haas S, et al. Incorporation of tetanus-epitope into virus-like particles achieves vaccine responses even in older recipients in models of psoriasis, Alzheimer's and cat allergy. *NPJ Vaccines.* 2017;2:30.
16. Bessa J, Kopf M, Bachmann MF. Cutting edge: IL-21 and TLR signaling regulate germinal center responses in a B cell-intrinsic manner. *J Immunol.* 2010;184(9):4615-9.
17. Bachmann MF, Zeltins A, Kalnins G, Balke I, Fischer N, Rostaher A, et al. Vaccination against IL-31 for the treatment of atopic dermatitis in dogs. *J Allergy Clin Immunol.* 2018;142(1):279-81 e1.
18. Fettelschoss-Gabriel A, Fettelschoss V, Thoms F, Giese C, Daniel M, Olomski F, et al. Treating insect-bite hypersensitivity in horses with active vaccination against IL-5. *J Allergy Clin Immunol.* 2018;142(4):1194-205 e3.
19. Zha L, Hongxin Z, Mohsen MO, Hong L, Zhou Y, Chen H, et al. Development of a vaccine against the newly emerging COVID-19 virus based on the receptor binding domain displayed on virus-like particles. *BioRxiv.* 2020.
20. Zha L, Chang X, Zhao H, Mohsen MO, Hong L, Zhou Y, et al. Development of a Vaccine against SARS-CoV-2 Based on the Receptor-Binding Domain Displayed on Virus-Like Particles. *Vaccines (Basel).* 2021;9(4).
21. Krueger CC, Thoms F, Keller E, Leoratti FMS, Vogel M, Bachmann MF. RNA and Toll-Like Receptor 7 License the Generation of Superior Secondary Plasma Cells at Multiple Levels in a B Cell Intrinsic Fashion. *Front Immunol.* 2019;10:736.
22. Organization WH. Temperature sensitivity of vaccines 2006 [Available from: <https://apps.who.int/iris/handle/10665/69387>].
23. Wang J, Peng Y, Xu H, Cui Z, Williams RO, 3rd. The COVID-19 Vaccine Race: Challenges and Opportunities in Vaccine Formulation. *AAPS PharmSciTech.* 2020;21(6):225.
24. Polack FP, Hoffman SJ, Crujeiras G, Griffin DE. A role for nonprotective complement-fixing antibodies with low avidity for measles virus in atypical measles. *Nat Med.* 2003;9(9):1209-13.
25. Klasse PJ. How to assess the binding strength of antibodies elicited by vaccination against HIV and other viruses. *Expert Review of Vaccines.* 2016;15(3):295-311.
26. Tay MZ, Poh CM, Renia L, MacAry PA, Ng LFP. The trinity of COVID-19: immunity, inflammation and intervention. *Nat Rev Immunol.* 2020;20(6):363-74.
27. Bachmann MF, Mohsen MO, Zha L, Vogel M, Speiser DE. SARS-CoV-2 structural features may explain limited neutralizing-antibody responses. *NPJ Vaccines.* 2021;6(1):2.
28. Hazenbos WL, Heijnen IA, Meyer D, Hofhuis FM, Renardel de Lavalette CR, Schmidt RE, et al. Murine IgG1 complexes trigger immune effector functions predominantly via Fc gamma RIII (CD16). *J Immunol.* 1998;161(6):3026-32.
29. Canton R, De Lucas Ramos P, Garcia-Botella A, Garcia-Lledo A, Gomez-Pavon J, Gonzalez Del Castillo J, et al. New variants of SARS-CoV-2. *Rev Esp Quimioter.* 2021.
30. Chang X, Augusto GS, Liu X, Kundig TM, Vogel M, Mohsen MO, et al. BNT162b2 mRNA COVID-19 vaccine induces antibodies of broader cross-reactivity than natural infection, but recognition of mutant viruses is up to 10-fold reduced. *Allergy.* 2021.
31. Harvey WT, Carabelli AM, Jackson B, Gupta RK, Thomson EC, Harrison EM, et al. SARS-CoV-2 variants, spike mutations and immune escape. *Nat Rev Microbiol.* 2021.

32. Bosnjak B, Stein SC, Willenzon S, Cordes AK, Puppe W, Bernhardt G, et al. Low serum neutralizing anti-SARS-CoV-2 S antibody levels in mildly affected COVID-19 convalescent patients revealed by two different detection methods. *Cell Mol Immunol.* 2021;18(4):936-44.
33. Sparrow E, Wood JG, Chadwick C, Newall AT, Torvaldsen S, Moen A, et al. Global production capacity of seasonal and pandemic influenza vaccines in 2019. *Vaccine.* 2021;39(3):512-20.
34. Rts SCTP. Efficacy and safety of RTS,S/AS01 malaria vaccine with or without a booster dose in infants and children in Africa: final results of a phase 3, individually randomised, controlled trial. *Lancet.* 2015;386(9988):31-45.
35. Bachmann MF, Mohsen MO, Zha LS, Vogel M, Speiser DE. SARS-CoV-2 structural features may explain limited neutralizing-antibody responses. *Npj Vaccines.* 2021;6(1).
36. Huang Y, Yang C, Xu XF, Xu W, Liu SW. Structural and functional properties of SARS-CoV-2 spike protein: potential antiviral drug development for COVID-19. *Acta Pharmacol Sin.* 2020;41(9):1141-9.
37. Liu X, Chang X, Rothen D, Derveni M, Krenger P, Roongta S, et al. AP205 VLPs Based on Dimerized Capsid Proteins Accommodate RBM Domain of SARS-CoV-2 and Serve as an Attractive Vaccine Candidate. *Vaccines (Basel).* 2021;9(4).
38. Balke I, Zeltins A. Use of plant viruses and virus-like particles for the creation of novel vaccines. *Adv Drug Deliver Rev.* 2019;145:119-29.
39. Sterlin D, Mathian A, Miyara M, Mohr A, Anna F, Claer L, et al. IgA dominates the early neutralizing antibody response to SARS-CoV-2. *Sci Transl Med.* 2021;13(577).
40. Bessa J, Zabel F, Link A, Jegerlehner A, Hinton HJ, Schmitz N, et al. Low-affinity B cells transport viral particles from the lung to the spleen to initiate antibody responses. *Proc Natl Acad Sci U S A.* 2012;109(50):20566-71.
41. Rodriguez A, Tjarnlund A, Ivanji J, Singh M, Garcia I, Williams A, et al. Role of IgA in the defense against respiratory infections IgA deficient mice exhibited increased susceptibility to intranasal infection with Mycobacterium bovis BCG. *Vaccine.* 2005;23(20):2565-72.
42. Vogel M, Augusto GS, Chang X, Liu X, Speiser D, Mohsen MO, et al. Molecular definition of SARS-CoV-2 RBD mutations: receptor affinity versus neutralization of receptor interaction. *Allergy.* 2021.
43. Brigger D, Horn MP, Pennington LF, Powell AE, Siegrist D, Weber B, et al. Accuracy of serological testing for SARS-CoV-2 antibodies: First results of a large mixed-method evaluation study. *Allergy.* 2021;76(3):853-65.

Figures legends:

Figure 1. CuMV_{TT}-VLPs constitute an efficient platform for genetically fusing the receptor-binding domain (RBM)

A, schematic depiction of *E. coli* cells containing pETDuet-1-derived plasmid, allowing the coexpression of CuMV_{TT}-RBM fusion and unmodified CMV_{TT} genes and production of mosaic VLPs termed (mCuMV_{TT}-RBM), B, SDS-PAGE analysis of the production and sucrose gradient purification of mCuMV_{TT}-RBM. M – protein size marker (Thermo Scientific), 0 – total proteins in *E. coli* C2566 cells before IPTG induction; T – total proteins in *E. coli* C2566 cells after IPTG induction and 18h cultivation at 20°C; S – soluble proteins in *E. coli* C2566 cells after induction and 18 h cultivation; P – insoluble proteins in *E. coli* C2566 cells after induction and cultivation; 60 – 0 – sucrose gradient fractions after separation of cell lysate in Beckman SW32 rotor; mCuMV_{TT}-RBM VLP containing sucrose fractions are labeled with red circle; C, native agarose gel analysis of the sucrose gradient fractions after sucrose gradient purification of mCuMV_{TT}-RBM. M – DNA size marker (Thermo Scientific), 60–0– sucrose gradient fractions after separation of the cell lysate in Beckman SW32 rotor; mCuMV_{TT}-RBM VLP containing sucrose fractions are labeled with

red circle; D, SDS-PAGE analysis of purified mCuMV_{TT}-RBM VLPs. M – protein size marker (Thermo Scientific), asterisk (blue) refers to unmodified CuMV_{TT} monomer and asterisk (green) refers to genetically modified CuMV_{TT}-RBM E, Electron microscopy analysis of purified mCuMV_{TT}-RBM VLPs; F, Dynamic light scattering analysis of purified mCuMV_{TT}-RBM VLPs. G, ACE2 binding to mCuMV_{TT}-RBD vaccine candidate, CuMV_{TT} and RBD alone were used as controls. Plates coated with 1µg/ml of ACE2. Binding was revealed using anti-CuMV mAb. One representative of 2 similar experiments is shown.

Figure 2: mCuMV_{TT}-RBM induces high levels of specific antibodies with high avidity against RBD and Spike proteins of SARS-CoV-2

A, Vaccination regimen D0/14 or D0/28 and bleeding schedule. B, RBD-specific IgG titer for the groups vaccinated with CuMV_{TT} as a control or mCuMV_{TT}-RBM on days 7, 14, 21, 28, 35 and 42 measured by ELISA OD₄₅₀. C, Log OD₅₀ of RBD-specific IgG titer for the group vaccinated with mCuMV_{TT}-RBM on days 7, 14, 21, 28, 35 and 42 (Data from B). D, Spike-specific IgG titer for the groups vaccinated with CuMV_{TT} as a control or mCuMV_{TT}-RBM on days 7, 14, 21, 28, 35 and 42 measured by ELISA OD₄₅₀. E, Log OD₅₀ of spike-specific IgG titer for the group vaccinated with mCuMV_{TT}-RBM on days 7, 14, 21, 28, 35 and 42 (Data from D). F, Avidity of RBD-specific IgG titer in mice vaccinated with mCuMV_{TT}-RBM using D0/14 vaccination regimen, sera were treated with PBST or 7M Urea. G, Avidity of RBD-specific IgG titer in mice vaccinated with mCuMV_{TT}-RBM using D0/28 vaccination regimen, sera were treated with PBST or 7M Urea. H, Avidity index of RBD-specific IgG in mice vaccinated with mCuMV_{TT}-RBM using D0/14 vaccination regimen, sera were treated with PBST or 7M Urea. L, RBD-specific IgG titer for the group vaccinated with mCuMV_{TT}-RBM on days 42 and 134. M, Spike-specific IgG titer for the group vaccinated with mCuMV_{TT}-RBM on days 42 and 134. Statistical analysis (mean ± SEM) using *Students t-test*, n=10. One representative of 3 similar experiments is shown. The value of $p < 0.05$ was considered statistically significant (* $p < 0.01$, ** $p < 0.001$, *** $p < 0.0001$).

Figure 3. mCuMV_{TT}-RBM promotes IgA production and IgG responses are dominated with IgG2a subclass

A, RBD-specific IgG titer for the groups vaccinated with CuMV_{TT} as a control and mCuMV_{TT}-RBM vaccine candidate on days 7, 14, 21 and 42 measured by ELISA by ELISA OD₄₅₀. B, Log OD₅₀ of RBD-specific IgG titer for the groups vaccinated with CuMV_{TT} as a control and mCuMV_{TT}-RBM vaccine candidate on days 7, 14, 21 and 42 (Data from A). C, Spike-specific IgG titer for the groups vaccinated with CuMV_{TT} as a control and mCuMV_{TT}-RBM vaccine candidate on days 7, 14, 21 and 42 measured by ELISA OD₄₅₀. D, Log OD₅₀ of spike-specific IgG titer for the groups vaccinated with CuMV_{TT} as a control and mCuMV_{TT}-RBM vaccine candidate on days 7, 14, 21 and 42 (Data from C). CuMV_{TT} $n=5$ and mCuMV_{TT}-RBM $n=10$. E, RBD-specific IgA titer for the groups vaccinated with CuMV_{TT} as a control and mCuMV_{TT}-RBM vaccine candidate using D0/D14 and D0/D28 regimens, measured by ELISA OD₄₅₀. F, Log OD₅₀ of RBD-specific IgA titer for the groups vaccinated with CuMV_{TT} as a control and mCuMV_{TT}-RBM vaccine candidate using D0/D14 and D0/D28 regimens, sera of day 35 was used. CuMV_{TT} $n=5$ and mCuMV_{TT}-RBM $n=5$. Statistical analysis (mean ± SEM) using *Student's t-test*. One representative of 3 similar experiments is shown. The value of $p < 0.05$ was considered statistically significant (* $p < 0.01$, ** $p < 0.001$, *** $p < 0.0001$).

Figure 4. Recognition of SARS-CoV-2 variants of concern (VoC)

A, RBD-specific IgG titers for the group vaccinated with mCuMV_{TT}-RBM measured by ELISA OD₄₅₀. B, Log OD₅₀ of RBD-specific IgG titer for the group vaccinated with mCuMV_{TT}-RBM (data from A). ELISA plates were coated with either RBD_{wildtype}, RBD_{K417N}, RBD_{E484K}, RBD_{N501Y}, RBD_{K417N/E484K/N501Y} or RBD_{L452R/E484Q}. Statistical analysis (mean ± SEM) *One-way ANOVA*, $n=5$. One representative of 2 similar experiments is shown. The value of $p < 0.05$ was considered statistically significant (* $p < 0.01$, ** $p < 0.001$, *** $p < 0.0001$).

Figure 5. mCuMV_{TT}-RBM induces higher antibody titers in comparison to SARS-CoV-2 convalescent sera

A, RBD-specific IgG titer for mice sera on D14 after priming with mCuMV_{TT}-RBM and COVID-19 convalescent sera (total 5 sera) measured with OD₄₅₀. B, RBD-specific IgG titer for mice sera on D28 after priming with mCuMV_{TT}-RBM and COVID-19 convalescent sera (total 5 sera) measured with OD₄₅₀. C, Area under curve (AUC) for RBD-specific IgG titer for mice sera on D14 after priming with mCuMV_{TT}-RBM and COVID-19 convalescent sera (total 5 sera). D, Area under curve (AUC) for RBD-specific IgG titer for mice sera on D28 after priming with mCuMV_{TT}-RBM and COVID-19 convalescent sera (total 5 sera). Statistical analysis (mean ± SEM) using *Student's t-test*, $n=5$. One representative of 2 similar experiments is shown. The value of $p < 0.05$ was considered statistically significant ($*p < 0.01$, $**p < 0.001$, $***p < 0.0001$).

Figure 6. Administration of a second booster dose further enhances antibody response and neutralization capacity of mCuMV_{TT}-RBM

A, Vaccination regimen D0/28 or D0/28/D49 and bleeding schedule. B, RBD-specific IgG titer for the groups vaccinated with mCuMV_{TT}-RBM vaccine candidate on day 14 (after prime), day 42 (after 2nd dose) and day 63 (after 3rd dose) measured by ELISA OD₄₅₀. C, Log OD₅₀ of RBD-specific IgG titer for the groups vaccinated with mCuMV_{TT}-RBM vaccine candidate on day 14 (after prime), day 42 (after 2nd dose) and day 63 (after 3rd dose) (Data from B). D, Avidity of RBD-specific IgG titer in mice vaccinated with mCuMV_{TT}-RBM on day 42 (after 2nd dose) and day 63 (after 3rd dose) measured by ELISA OD₄₅₀, sera were treated with PBST or 7M Urea. E, Log OD₅₀ of RBD-specific IgG titer in mice vaccinated with mCuMV_{TT}-RBM on day 42 (after 2nd dose) and day 63 (after 3rd dose) (data from D). F, Neutralization titer (CPE) for sera from CuMV_{TT} control group, day 42 (after 2nd dose) and day 63 (after 3rd dose). Statistical analysis (mean ± SEM) using *Students t-test*, $n=5$. One representative of 2 similar experiments is shown. The value of $p < 0.05$ was considered statistically significant ($*p < 0.01$, $**p < 0.001$, $***p < 0.0001$).

Figure 7. Efficient upscaling of mCuMV_{TT}-VLPs vaccine candidate

A, A sketch illustrating the upscale production of mCuMV_{TT}-VLPs vaccine candidate. B, SDS-PAGE; C, Agarose gel and D, Dynamic light scattering (DLS) analysis of purified mCuMV_{TT}-RBM vaccine.

Supplementary Figure 1

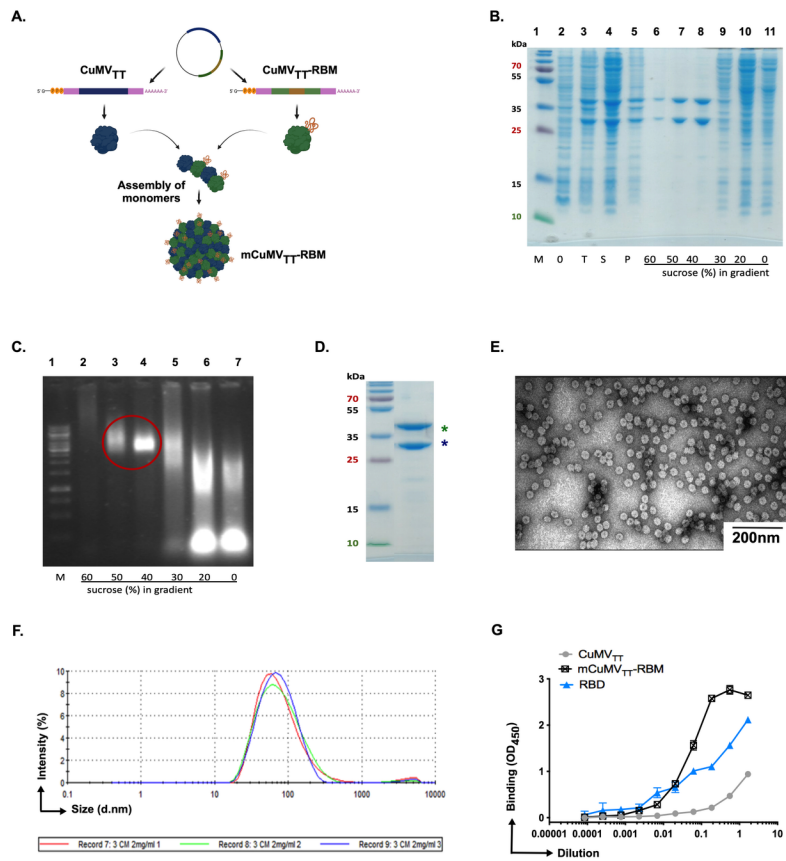
A and D, SDS-PAGE; B and E, Agarose gel; C and F, Dynamic light scattering (DLS) analysis of mCuMV_{TT}-RBM vaccine. Vaccine sample was analyzed directly after production and after 14 month storage at 4°C. The asterisk in (blue) is unmodified CuMV_{TT} monomer and the asterisk in (green) is genetically modified CuMV_{TT}-RBM.

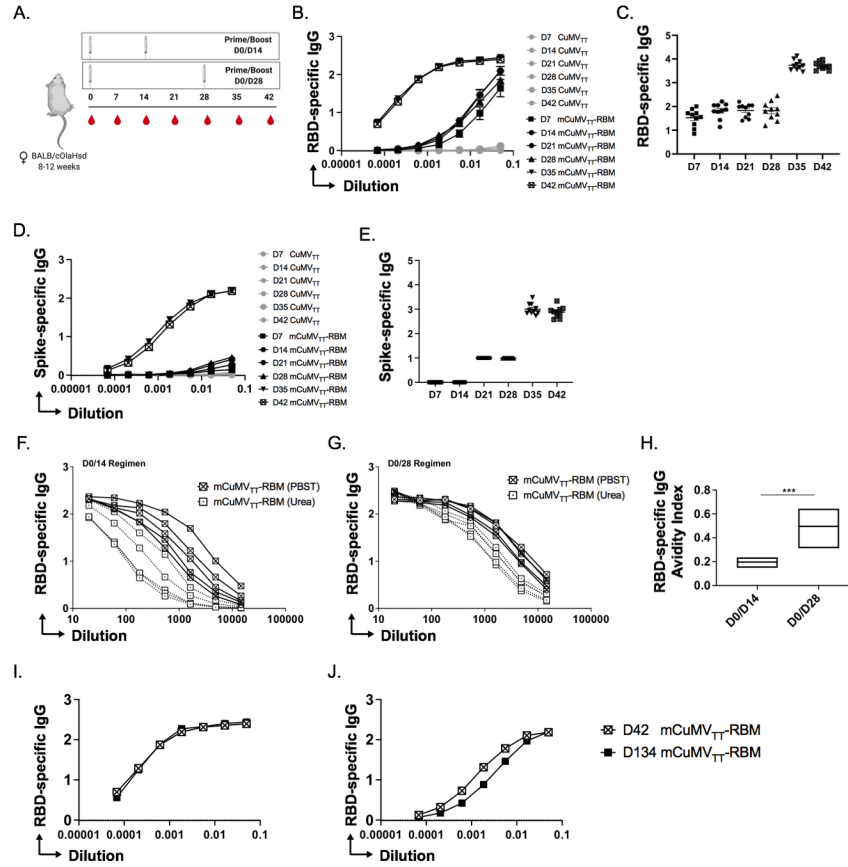
Supplementary Figure 2

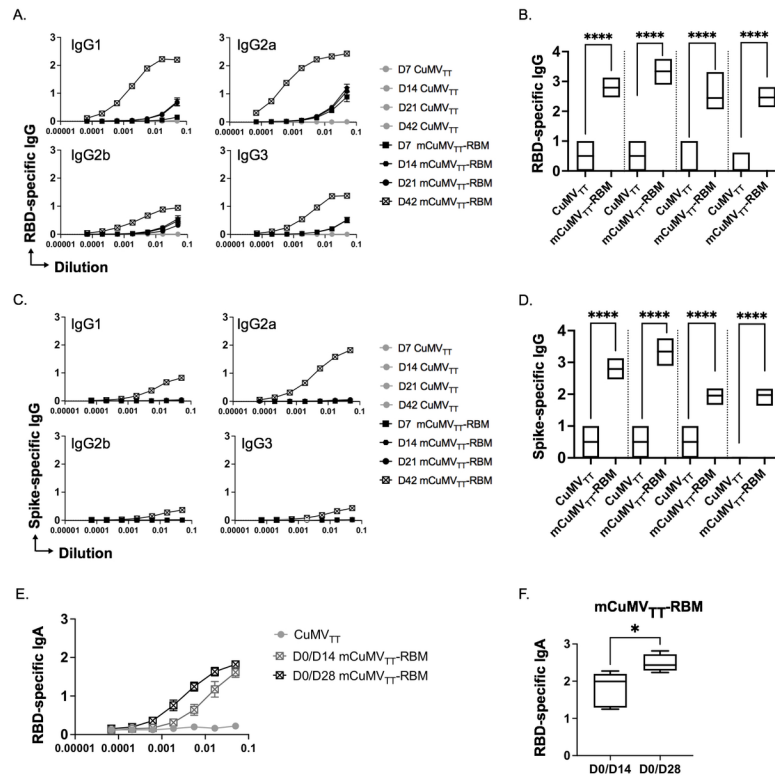
A, Avidity of spike-specific IgG titer in mice vaccinated with mCuMV_{TT}-RBM using D0/14 vaccination regimen, sera were treated with PBST or 7M Urea. B, Avidity of spike-specific IgG titer in mice vaccinated with mCuMV_{TT}-RBM using D0/28 vaccination regimen, sera were treated with PBST or 7M Urea. C, Avidity index of spike-specific IgG in mice vaccinated with mCuMV_{TT}-RBM using D0/14 vaccination regimen, sera were treated with PBST or 7M Urea. Statistical analysis (mean ± SEM) using *Student's t-test*, $n=10$. One representative of 2 similar experiments is shown. The value of $p < 0.05$ was considered statistically significant ($*p < 0.01$, $**p < 0.001$, $***p < 0.0001$).

Supplementary Figure 3

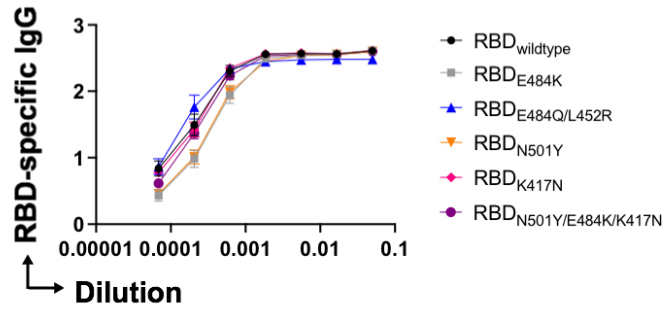
RBD-specific IgG titer for the rabbit's groups vaccinated with CuMV_{TT} as a control or mCuMV_{TT}-RBM on day 42 measured by ELISA (Log OD₅₀ in C: given as reciprocal dilution values). Males $n=2$ control and $n=3$ vaccinated – Females $n=3$ control and $n=3$ vaccinated. Statistical analysis (mean ± SEM) using *Students' t-test*. The value of $p < 0.05$ was considered statistically significant ($*p < 0.01$, $**p < 0.001$, $***p < 0.0001$).







A.



B.

